Structural characterization of water/ice formation in SBA-15 silicas: III. The triplet profile for 86 Å pore diameter

2008 J. Phys.: Condens. Matter 20 205108

(http://iopscience.iop.org/0953-8984/20/20/205108)

J. Phys.: Condens. Matter **20** (2008) 205108 (12pp) doi:10.1088/0953-8984/20/20/205108

Structural characterization of water/ice formation in SBA-15 silicas: III. The triplet profile for 86 Å pore diameter

J Seyed-Yazdi[1,2], H Farman[1], John C Dore[2], J Beau W Webber[2,3,4] and G H Findenegg[5]

[1] Iran University of Science and Technology, Narmak, Tehran, Iran
[2] School of Physical Sciences, University of Kent, Canterbury, CT2 7NH, UK
[3] Institute of Petroleum Engineering, Heriot Watt, Edinburgh EH14 4AS, UK
[4] Lab-Tools Ltd, G17 Canterbury Enterprise Hub, University of Kent, CT2 7NJ, UK
[5] Department of Chemistry, Technical University Berlin, Strasse des 17 Juni 124, D-10623 Berlin, Germany

E-mail: J.C.Dore@kent.ac.uk

Received 12 November 2007, in final form 7 April 2008
Published 1 May 2008
Online at stacks.iop.org/JPhysCM/20/205108

Abstract

The diffraction results for the formation of ice in 86 Å diameter pores of a SBA-15 silica sample are analysed to provide information on the characteristics of the ice created in the pores. The asymmetric triplet at ∼1.7 $Å^{-1}$, which involves several overlapping peaks, is particularly relevant to the different ice phases and contains a number of components that can be individually identified. The use of a set of three peaks with an asymmetric profile to represent the possibility of facetted growth in the pores was found to give an unsatisfactory fit to the data. The alternative method involving the introduction of additional peaks with a normal symmetric profile was found to give excellent fits with five components and was the preferred analytic procedure. Three peaks could be directly linked to the positions for the triplet of hexagonal ice, I_h, and one of the other two broad peaks could be associated with a form of amorphous ice. The variation of the peak intensity (and position) was systematic with temperature for both cooling and heating runs. The results indicate that a disordered state of ice is formed as a component with the defective crystalline ices. The position of a broad diffraction peak is intermediate between that of high-density and low-density amorphous ice. The remaining component peak is less broad but does not relate directly to any of the known ice phases and cannot be assigned to any specific structural feature at the present time.

1. Introduction

In the preceding paper (Seyed-Yazdi *et al* 2008a), called Paper 2, the data obtained for neutron diffraction from ice nucleation in an 'almost-filled' sample of SBA-15 silica with a pore diameter of 86 Å has been presented for a wide range of temperatures and for two different cooling/heating rates. The overall results are similar to those obtained in earlier studies (Baker *et al* 1997, Webber and Dore 2004, Liu *et al* 2006) of ice nucleation in mesoporous silicas. However, the use of a longer wavelength for the incident neutron beam gives a better Q-resolution and consequently allows a more precise analysis of the peak profiles. The ice triplet centred at ∼1.7 $Å^{-1}$ is of particular interest in this context. The previous work on ice formed in mesoscopic pores has always displayed an asymmetric profile that has been associated with the presence of some defect or disorder in the confined ice structure. The present measurements enable a more complete analysis of the diffraction pattern to be undertaken using curve-fitting techniques. The results allow an interpretation of the co-existing phases of ice formed in the pores. A previous paper (Liu *et al* 2006), Paper 1 in the series, has presented data for the 'over-filled' case using the same sample material and identical experimental conditions. Paper 2 presents a general analysis of the 'almost-full' case and the present paper examines the triplet profile for this situation in a more quantitative manner.

2. Profile analysis

2.1. Experimental results

The measurements were made on the D20 diffractometer at the Institut Laue Langevin for several SBA-samples. The fabrication details and the experimental procedure have been presented in Paper 1 of this series (Liu *et al* 2006). The main feature addressed in the current paper is the data covering the Q-range, 1.5–2.1 Å^{-1}. This region would normally have three well-defined peaks for hexagonal ice or a single central peak for cubic ice. However, the diffraction pattern has a complex shape, which seems to retain the same general profile over a wide temperature range despite a significant change in its intensity.

The overall appearance of the profile suggests that the Bragg peaks are markedly asymmetric with a sharp rise on the low-Q side and a long tail on the high-Q side, as reported in the earlier studies (Webber and Dore 2004) for a range of porous silicas. However, the peaks are also strongly overlapping, so the true nature of the individual profiles is masked by the presence of adjacent peaks. Furthermore, the peak profile appears to be variable according to the sample material and displays significant variation due to pore size and network type (i.e. sol–gel, CPG, MCM/SBA, etc). The shape is particularly dependent on the fractional filling-factor for the pores. Previous neutron diffraction measurements (Baker *et al* 1997) for a range of pore sizes and pore fillings have emphasized the significant variations that can occur in the shape of the diffraction pattern for this Q-value range. The systematic work of Morishige using x-ray diffraction (Morishige and Uematsu 2005) with a range of different mesoporous silicas is also of particular interest in this respect and is complementary to the neutron studies, as although the crystalline components will be similar, the disordered components will be different.

A change in the pore volume and the filling-factor can also have a direct influence on the observed scattering distribution through the phenomenon of diffraction broadening, which is particularly important for small pore dimensions. The first discussion of the effect was presented in the early work with sol–gel silicas (Steytler *et al* 1983a, Steytler and Dore 1985). Under these circumstances, it may become difficult to isolate the effects resulting from the restricted dimensions of the water/ice component from a real variation in its structural characteristics on a molecular scale. This effect was of minor importance in the earlier studies made with a liquids diffractometer but becomes more significant in the present measurements. Another important issue is the apparent presence of a diffuse scattering contribution under the Bragg peaks that is not normally considered in the analysis procedure for ice formed under these conditions, although its presence was noted in the first identification of cubic ice in porous silicas (Steytler *et al* 1983b). Furthermore it seems that the disordered component may dominate for situations where the water/ice coverage is low (Zanotti *et al* 2005). Consequently, it is interesting to use the data presented in Paper 2 for a Q-range of 1.5–2.1 Å^{-1} to make a more detailed study of the different ice phases.

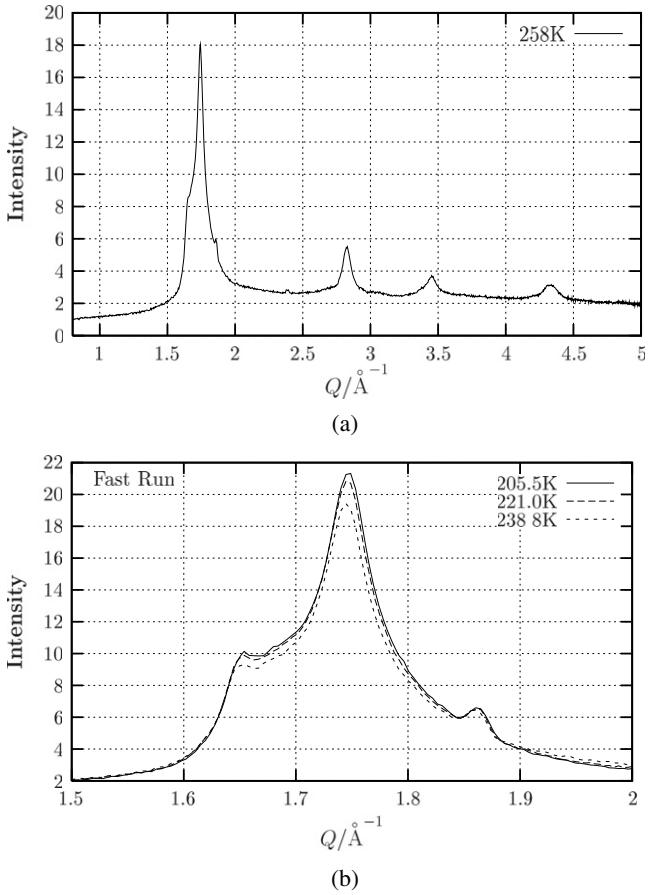

Figure 1. (a) The full diffraction pattern for water/ice in 86 Å pores at 258 K, (b) the profile of the main diffraction peaks at various temperatures.

2.2. Asymmetric peak profile analysis

The overall diffraction pattern for the full Q-range of the measurement is shown in figure 1(a) at 258 K and the intensity profile in the region of 1.7 Å^{-1} is shown in figure 1(b) for a range of different temperatures. The pattern for 1.5–2.0 Å^{-1} seems to resemble that of hexagonal ice with a triplet of peaks corresponding to the [100], [002] and [101] reflections. However, the widths of the peaks are much broader than those observed for the hexagonal ice formed on the outside of the silica grains, (Liu *et al* 2006).

It is also clear that the central peak is enhanced relative to the other peaks and this is due to the presence of cubic ice, which has only a single peak at the centre of the triplet distribution. The profile therefore seems to be a hybrid of both hexagonal and cubic ice forms. In earlier studies with sol–gel silicas, the cubic ice component was more dominant and consequently it has been usual to refer to the ice as 'defective cubic ice'. Subsequent work has emphasized the inter-relationship of the two ice forms and Morishige makes specific comment that it is preferable to describe the ice as 'defective hexagonal ice' (Morishige and Uematsu 2005). It is now widely assumed that the ice confined in the pores contains a large number of stacking faults (Kuhs 1998) so that it is probably more appropriate to refer to these ice phases simply

as 'defective ice-I', in which both cubic and hexagonal ice forms are incorporated. However, a detailed crystallographic analysis of this type of defective structure is complicated by the need to retain the hydrogen-bond connectivity in the three-dimensional ice structure and a treatment of this problem has only recently been attempted (Hansen *et al* 2007). The neutron measurements of Paper 2 show that the basic shape of this compound triplet profile remains approximately constant with respect to temperature but the intensity is seen to vary systematically over the whole range studied. Other recent work on partially-filled samples, that will be reported in subsequent papers (Seyed-Yazdi *et al* 2008b), indicates that there may be some minor differences in the temperature range just below the onset of nucleation.

The observation of a slowly-decaying intensity on the high Q-value side of the main triplet peak has been taken to be an indication of the presence of an asymmetric peak function that can be associated with a defective form of cubic (or hexagonal) ice. In fact, it seems that cubic ice is rarely, if ever, formed without some indication of a shoulder on the low-Q side of the central peak and a weakly-decaying 'tail' on the high-Q side. This asymmetric form immediately suggests a link to the Warren profile that was originally developed (Warren and Bodenstein 1965, 1966) for the description of certain forms of carbon. The essential features arise from the facetted growth of the crystal lattice along particular directions that, when averaged over all orientations for a powder sample, give rise to an asymmetric peak profile. The basic formalism proposed by Warren was subsequently developed by Ergun (Ergun 1970) and gives a good description of the observed diffraction patterns for materials such as activated carbons (Szczygielska *et al* 2001) In this case, the graphene sheet has long-range correlations in the plane of the sheet, whereas the number of well-correlated stacked layers is limited to a much shorter range. In effect, the crystallites display variable correlation features in different directions and the process of averaging over random orientations produces asymmetric peaks in the diffraction pattern.

Close examination of the total diffraction patterns shown in figures 1(a) and (b) indicates that there is also a diffuse scattering component present in the pattern, such that the overall level of scattering on the low-Q and high-Q sides of the main peaks has a different intensity. For the purpose of analysing the peak profiles, it is important to eliminate this contribution and consequently a smooth 'background' term has been fitted using a low-order polynomial, and then subtracted from the data, to give an isolated profile in which the asymptotic values approach zero on each side of the peaks.

2.3. Symmetric peak profile analysis

There are two approaches to the peak fitting process based on the use of either symmetric or asymmetric peak functions. A suitable mathematical expression for a symmetric peak function may be defined by the following expression:-

$$I(Q,i) = \frac{I_0(i)}{\cosh[(Q - Q_0(i))/\sigma(i)]} \qquad (1)$$

where $I(Q,i)$ is the intensity, $I_0(i)$ is the peak height, $Q_0(i)$ is the peak position and $\sigma(i)$ is a width parameter; the index, i, runs over the number of peaks in the composite function. This form was used in preference to the usual Gaussian function as it has a slightly broader spread in the wings. The basic principles of the method are not affected by the choice of this form, which was used in the analysis of the higher order peaks in the previous papers. The introduction of a skew effect for the three peaks is conveniently made by modifying this expression with the introduction of two additional parameters and is described in appendix A.

2.4. Multi-component peak analysis

An alternative view is that the ice created in the pores involves the presence of other forms of ice than simple cubic and hexagonal crystallites. In this context, there could be a contribution from highly defective or disordered forms of ice, so that the assembly should not be regarded simply as a homogeneous collection of crystallites with well-defined boundaries. In this case the profile is envisaged as a number of overlapping symmetrical peaks and a curve-fitting procedure is adopted to isolate the individual components. It was quickly established that only two additional broad peaks were necessary in addition to the well-recognised ice triplet, in order to obtain good fits to the data. The five peaks were defined in an equivalent way, using the symmetric 'sech' function defined by the expression given in equation (1); a similar fitting routine was used based now on one linear and two nonlinear parameters for each peak.

3. Results

3.1. Three asymmetric-component treatment

An early attempt to fit the neutron diffraction data to a medium-resolution profile was made by Baker (1996) for neutron studies of defective ice formation in a 60 Å sol–gel silica from Aldrich. The measurements (Baker 1996) were made on the G61 diffractometer of the Orphee reactor and gave a similar asymmetric shape to the present results showing a strong central peak. A formalism (Ergun 1970) based on a disc-shaped layer for the crystallite was used to represent the first peak, with Gaussian functions for the second and third peaks. Although the parameter fitting procedure was not exhaustive, it quickly became apparent that there were major problems in adequately representing the asymmetric profile with this combination of peaks.

The present data represent a more direct test for the fitting of asymmetric peaks using the formalism expressed in equation (1). The program, NONLINREG (Evans 1997) was used to obtain an optimal fit to the datafiles from the cooling run at the faster ramp rate. This set was used initially because the third peak, which has a small intensity, was more pronounced in these datafiles and could therefore provide a better definition of the parameter values, I_0, Q_0, ε^2, σ_ε and σ for each of the three peaks. There was some difficulty in obtaining good convergence for many of the runs and the fits were not of high quality. One of the best results was

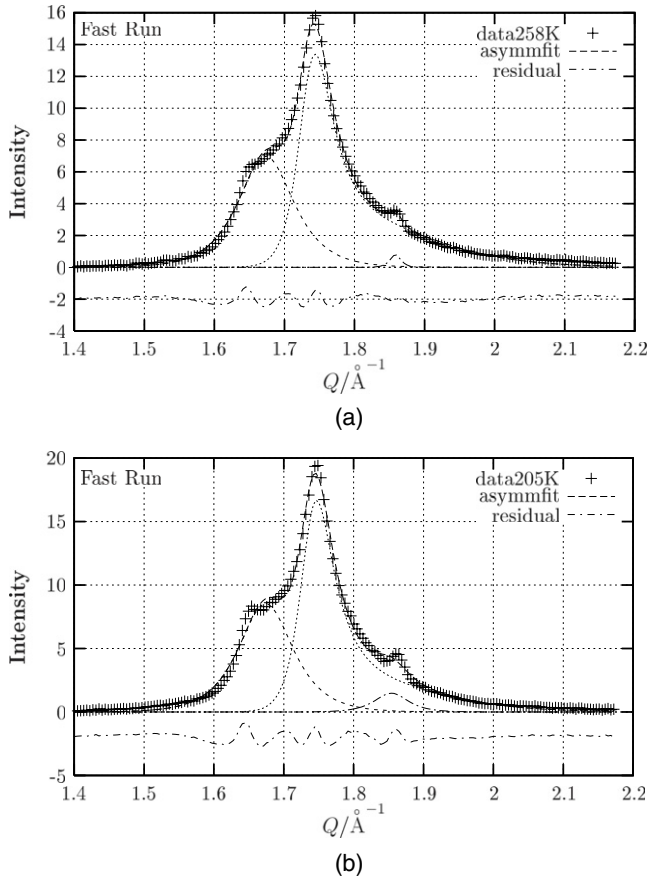

Figure 2. The fitted profile for the fast run using three asymmetric peak functions, (a) 258 K and (b) 205 K.

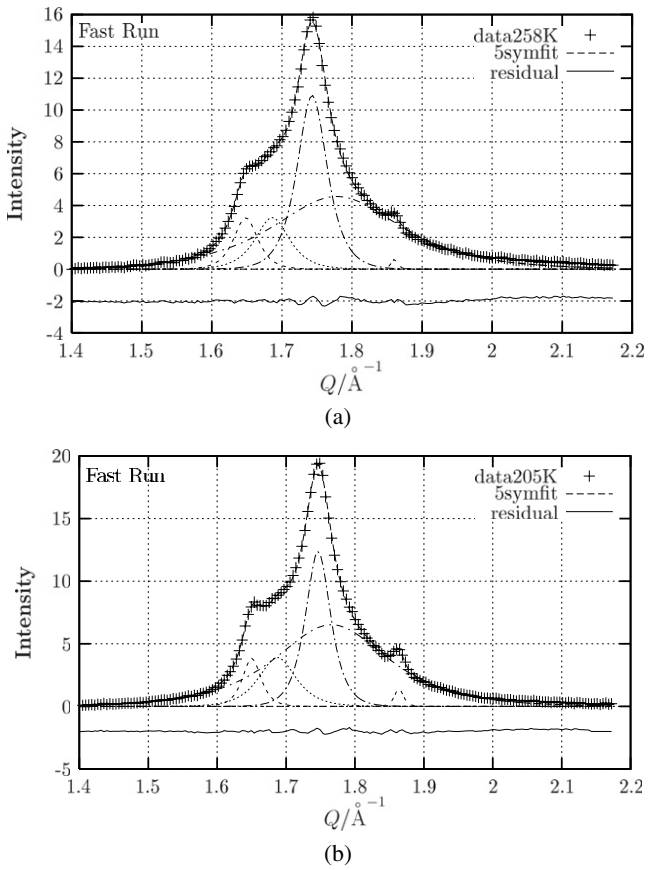

Figure 3. The fitted profile for the fast run using five symmetric peak functions, (a) 258 K and (b) 205 K.

obtained for the situation just after the onset of nucleation and a converged fit for 258 K is shown in figure 2(a). The minor third peak is seen to have little asymmetry and is quite well fitted but peaks 1 and 2 have a marked asymmetry. The residual function, shown beneath the main fit, indicates that the regions of the shoulder and the main peak have systematic variations and are not particularly well represented by the overall shape. The situation becomes more apparent at the lower temperatures as indicated in figure 2(b) for a temperature of 205 K. In this case the 'fit' is very poor despite having started from similar parameter values. It appears that the shape of the shoulder in the low-Q region is slightly different and the program produces a compromise fit with a shifted position for peak-1 that affects the shape of the central peak-2 and leads to complete failure to adequately represent peak-3. The goodness of fit parameter is clearly worse than that obtained for the fit to the 258 K profile even though it represents the optimal values of the parameters.

Several other tests were made in which the small peak-3 was first subtracted from the dataset and the program was used to represent the remaining profile with two asymmetric peaks, in order to avoid the behaviour shown in figure 2(b) but it was still not possible to obtain a satisfactory fit. It was concluded that the shape of the shoulder on the low-Q side could not be adequately represented by a single peak superimposed on the side of the main peak and that an alternative formulation was needed.

3.2. Five symmetric-component treatment

There are three clearly-identified features that indicate the presence of peaks that are readily associated with the normal triplet features of hexagonal ice. The fact that they are broadened relative to the behaviour of bulk hexagonal ice (Liu *et al* 2006) is not surprising because the crystallites are restricted in size and some diffraction broadening will occur. However, the high Q-value region displays a broad 'tail' with a much larger apparent width and the small, relatively-sharp peak-3 superimposed on the falling intensity, making it difficult to estimate the width of the central peak. It was decided to incorporate additional symmetric peaks to represent the overall peak profile, and as a method of obtaining a reliable value for the width of this central peak. The NONLINREG program was again used with the defining function specifying five symmetric functions as given in section 2.3 and equation (1). Although the number of free parameters was initially similar to the fits with three asymmetric functions, a much improved fit was quickly obtained, confirming that only five peaks were needed. The converged fits to the 258 and 205 K datasets are shown in figures 3(a) and (b); the residual functions, shown below, are clearly improved over the previous analysis. The positions of the peaks for the known ice triplet were found to be in the correct ratios despite being allowed a free variation during the initial searches. The shape of the shoulder in the low-Q region seems to require an additional broad peak that occurs between

peak-1 and peak-2 of the ice triplet and the fall-off region on the high-Q side requires a broad peak centred between peak-2 and peak-3 of the ice triplet. Furthermore, this scheme of three relatively-sharp peaks and two broadened peaks is capable of fitting all the datafiles, covering the whole of the temperature range studied. It therefore seems clear that these two additional peaks are needed to fully represent the observed profile and to obtain a systematic variation of the parameters. In this context, it becomes necessary to re-label the peaks sequentially with peaks 1, 3 and 5 as the ice triplet and peaks 2 and 4 as the slightly broadened and significantly broadened additional peaks; this notation is used for the remaining part of the paper.

The results for the slow run have greater statistical accuracy per temperature interval than the fast run and therefore lead to a larger number of data points in both the cooling and heating runs. The results for the slow run also show a smaller magnitude for peak-5. Corresponding fits for these datasets are given in figures 4(a)–(d), covering a wider temperature range. The five-component analysis routine again gives an excellent fit to the profile with a similar set of parameter values. It will be seen in the following section that there is a systematic variation of some parameter values with temperature, so the question posed by this scheme concerns the origin of the additional peaks. Peak 4 contributes the major part of the trailing part of the profile on the high-Q side that had led to the initial suggestion of asymmetry but can now be seen to be caused by the presence of a symmetric broad peak centred at 1.77 Å^{-1}. This feature immediately suggests the possibility of an amorphous ice component but the peak position for annealed low-density amorphous (lda) ice is at $Q_0 = 1.69$ Å^{-1} so there is no direct correspondence. The position of the main diffraction peak for high-density amorphous (hda) ice is at $Q_0 = 2.1$ Å^{-1} so the position is in between the two values. Koza *et al* (2006) have studied the transformation of hda ice to lda ice, which displays a range of intermediate states in which the diffraction peak moves to lower Q values as a function of time/temperature. It therefore seems feasible that there is a range of amorphous ice structures that correspond to intermediate density and a metastable network of hydrogen-bonds that are stabilized by the thermal history of the sample.

However, the study of ice formed on the surfaces of activated carbons (Bellissent-Funel *et al* 1996) is also relevant to this discussion. Measurements were made for water adsorbed into the mesopores of a high surface area carbon and measured for the liquid at room temperature and for ice at 77 K. If the hydration level was high the diffraction pattern showed the usual characteristics of hexagonal ice. However, for a lower coverage ($f = 0.25$), it was found that no crystalline material was formed when the sample was cooled to liquid nitrogen temperatures. The diffraction pattern showed a broad oscillatory structure with a distinct resemblance to lda ice but the main diffraction peak occurred at 1.85 Å^{-1} for $f = 0.25$ and 1.90 Å^{-1} for $f = 0.50$. More recent work for low coverage in a Vycor sample (Zanotti *et al* 2005) and a SPS silica sample (Jalassi *et al* 2008) has also given a similar behaviour. The conjunction of this peak with the position of peak-4 in the fits to the present data is suggestive of the formation of a glassy form of ice that is intermediate between

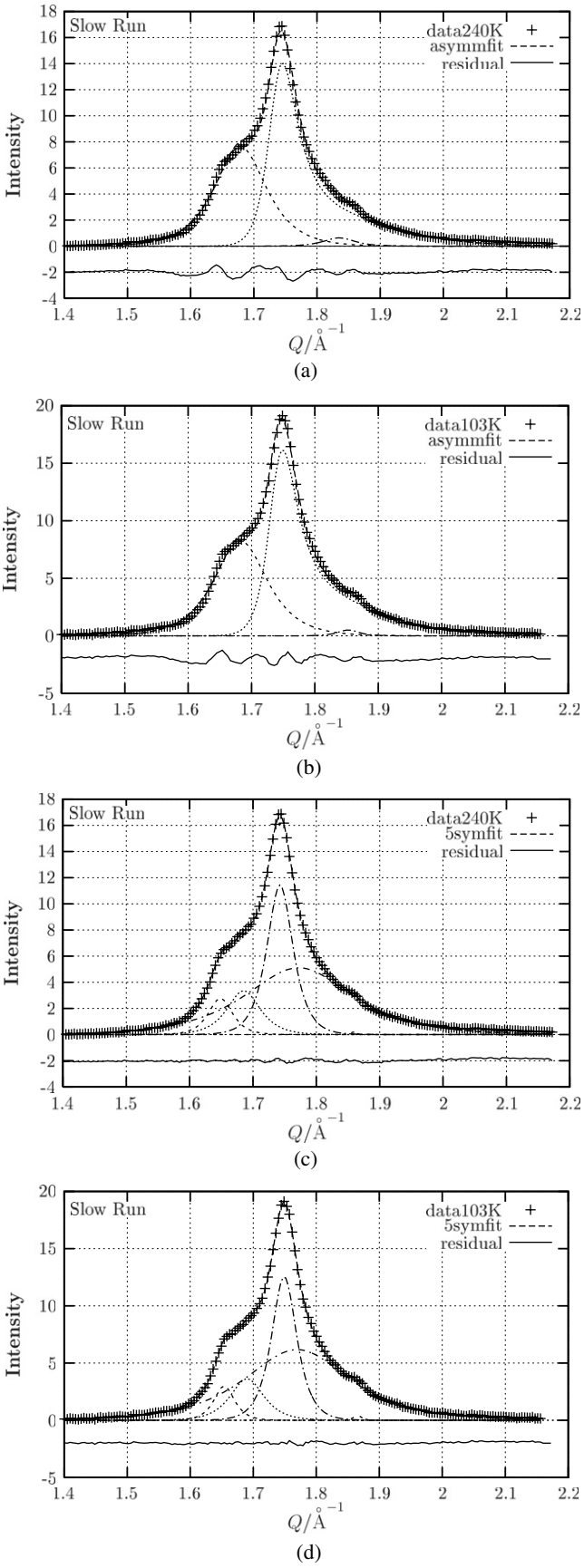

Figure 4. The fitted profile for the slow run, (a) 240 K three asymmetric peaks, (b) 103 K three asymmetric peaks, (c) 240 K five symmetric peaks and (d) 103 K five symmetric peaks.

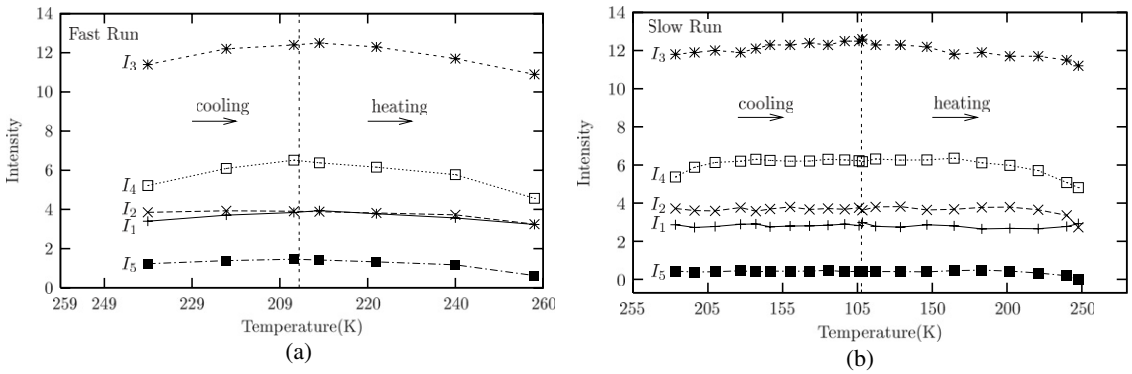

Figure 5. The intensity variation, $I_0(T)$, for the component peaks, (a) fast run, (b) slow run. (Note the different temperature range for the two cases.)

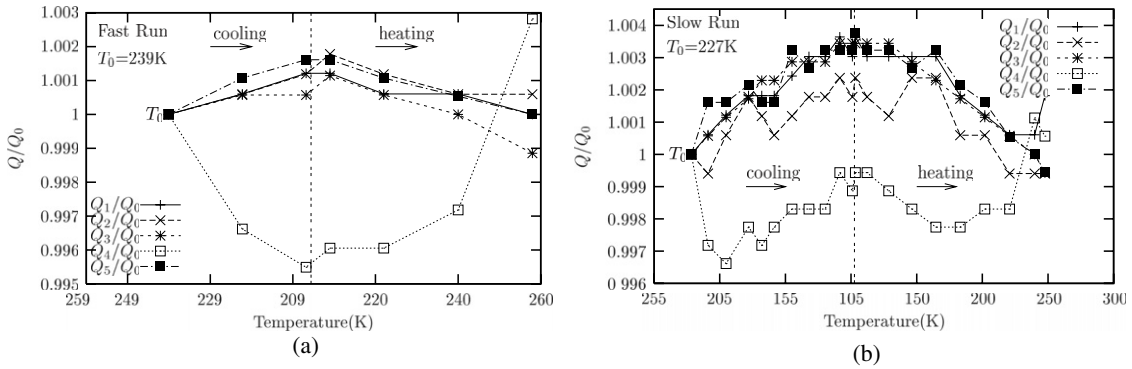

Figure 6. The relative shift function, $Q_0(T)/Q_0(T_{\text{ref}})$ for the parameter values shown in figure 5. (Note: a different T_0 is used and that the temperature scale covers a different range.)

lda and hda ice. This possibility is further explored in the next section (section 3.3).

3.3. Temperature variation of the parameter values

Although a free parameter search was adopted in all cases, the converged values of the various parameters show a consistent pattern. The most important parameter is I_0, which represents the height of the peaks, as the width parameter, σ, remains relatively constant. The integrated peak intensities depend on both I_0 (figures 5(a) and (b)) and σ for the cooling and heating sequence and the different rates of temperature change. It is immediately apparent that the contributions to all peaks rise with reducing temperature and decrease with rising temperature, as already apparent from the behaviour of the sample data shown in figure 4.

Over the range 259–208 K the increase corresponds to a change of 15% in the central peak height for the fast temperature change and 4% in the central peak height for the slow temperature change. Over the wider range 259–95 K the central peak height for the slow temperature change exhibits an 11% increase. However this also reveals that each component changes at a slightly different rate. The main feature is the totally reversible nature of the curve, as found in the earlier studies for water/ice in MCM materials (Dore *et al* 2004) and as mentioned in preliminary discussions for these SBA materials (Liu *et al* 2006, Webber *et al* 2007b). This lack of hysteresis is surprising and indicates that there is a metastable equilibrium between the different phases that varies with the absolute temperature. This behaviour is discussed further in section 4.

It is instructive to show the variation with reference to a fixed temperature T_{ref}. This temperature is chosen to be just below the measured temperature of nucleation—239 K in the fast run and 227 K in the slow run. The function $Q_0(T)/Q_0(T_{\text{ref}})$ is given in figures 6(a) and (b). In this context it becomes clear that peak-4 behaves in an anomalous manner and, although the shape is somewhat different for the 'fast' and 'slow' runs, it seems that there is an opposite displacement of the peak with respect to temperature. In effect the structural correlations giving rise to this peak appear to expand as the temperature is reduced. This behaviour is also discussed in section 4. The width parameters for each of the peaks remain fairly constant over the whole temperature range but have different values as shown in figure 7; the parameters for the five peaks, at 200 and 258 K, are given in table 1. The variation of the positions of the triplet peaks is given in figure 6. The ratio of the peak positions remains constant within 0.05% and the actual values for 205 and 258 K are listed in table 1. In the case of bulk ice the c/a ratio remains constant over a wide temperature range with a value of 1.628. The corresponding value for the confined ice is 1.637 which is a slight increase and presumably results from the defective nature of the ice in

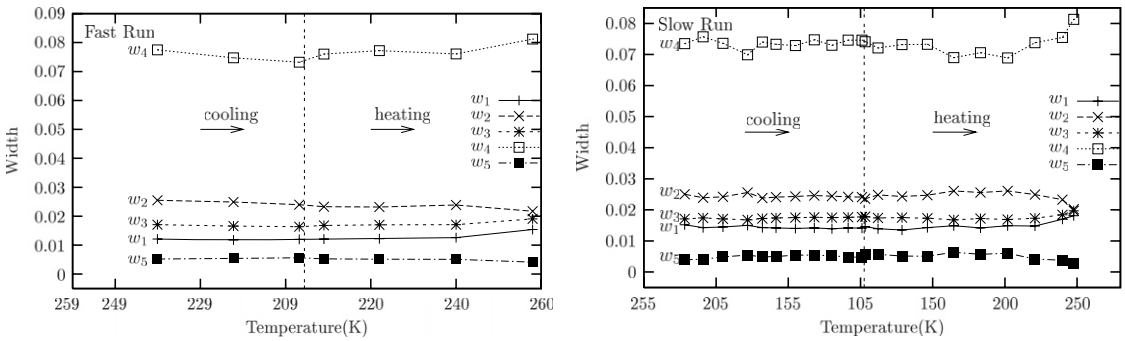

(a) (b)

Figure 7. The width parameter, $\sigma(T)$ (w(T) on graph), for the peaks, (a) fast run, (b) slow run.

Table 1. Peak parameters: amplitude, centre position Q_0, full-width-at-half-maximum, and Q_0/Q_0^{Pk3} for the five peaks, at 205 and 258 K.

Temperature (°C)	Peak No.	Amplitude (Å^{-1})	Q_0	FWHM (Å^{-1})	Q_0/Q_0^{Pk3}
	1	3.84	1.6502	0.032	0.9449
	2	3.90	1.6874	0.063	0.9661
205	3	12.36	1.7465	0.043	1
	4	6.52	1.7660	0.193	1.0112
	5	1.45	1.8638	0.015	1.0672
	1	2.80	1.6516	0.037	0.9450
	2	3.81	1.6878	0.064	0.9657
258	3	12.31	1.7477	0.046	1
	4	6.20	1.7682	0.192	1.0117
	5	4.24	1.8645	0.014	1.0668

the pores. It is notable that peak 5 for the 101 reflection is considerably sharper than the others and shows no additional broadening compared with that for the hexagonal ice formed on the outside of the grains. The other two peaks of the ice I_h triplet have comparable widths although the central peak (002) is always a little broader than the first peak (100).

4. Conclusions

4.1. Ice phases and stability

The results presented in section 3 indicate the presence of two different phases of ice, namely ice I_h with ice I_c (or a hybrid form of both structures) and an amorphous component that can be characterized as an intermediate density form of amorphous ice (ida ice). The distribution of these materials through the pore network is not defined by these measurements. It is therefore impossible to say whether there are regions in the pore volume that consist mainly of one form of ice or whether they are effectively mixed into a fairly homogeneous volume with a textural variation.

The three sharp peaks (1, 3, 5) correspond to the triplet peaks of ice I_h and the ratios for the peak positions correspond to the expected values. However, the intensity ratios do not correspond, as shown by comparison with the diffraction pattern for ice I_h formed on the outside of the pores (Liu *et al* 2006). The indication is that the crystalline component consists of a composite form of ice-I_c and ice-I_h, arising from stacking faults or some other variation that leads to the creation of a defective lattice structure.

The most interesting feature arising from the fitted curves is the presence of the broad peaks 2 and 4 and their systematic variation with temperature, as represented in figures 5 and 6 for $I_0(T)$ and $Q_0(T)/Q_0(T_{\rm ref})$. Peak-4 shows an anomalous behaviour as the displacement of the peak position, $Q_0(T)/Q_0(T_{\rm ref})$, which follows an opposite dependence on temperature to the other peaks. The shape of this function appears different in figures 6(a) and (b) for the slow and fast cooling runs but this is because a different temperature range is covered. It is clear from the cooling run that the peak moves initially to lower Q-values for the temperature range down to 200 K but at lower temperatures (<200 K) behaves in a similar manner to the other peaks.

It is noticeable from the total scattering pattern (figure 1(a)) that there is a disordered contribution that extends over the whole Q-range. This feature is most clearly shown by the difference in levels below and above the triplet peaks. In the peak analysis of section 3.3, this 'background' contribution has been removed to provide a suitable analysis procedure but it is seems likely that peak-4 is directly linked to this diffuse scattering contribution, which extends over the whole Q-range and is indicative of an amorphous ice form. Amorphous ice in the bulk form can be created by a number of different routes and it appears that there are possibly two distinctive states corresponding to low-density amorphous ice (lda) and high or very high-density amorphous ice (vhda); a brief summary of their characteristics and transformation properties is given in appendix B.

It would seem from the behaviour of the intensity of peak-4 curve (figures 5(a) and (b)) that this component is formed during the initial stages of the nucleation event and that a substantial proportion of the ice volume has these characteristics. All the peaks show an increase in amplitude at lower temperatures, but the fractional increase for peak-4 is substantially greater than for the other peaks. There is also a slight variation in the width parameter that also shows an decrease at low temperatures and could possibly be associated with a change in the spatial correlations of the disordered phase arising from restricted vibrational motion.

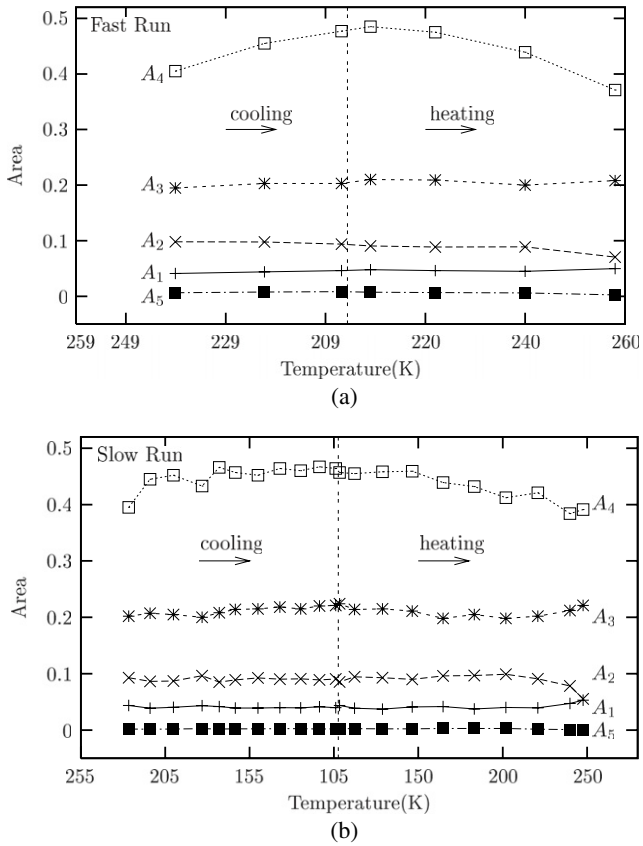

Figure 8. The peak areas, $A(T)$, for the peaks, (a) fast run, (b) slow run.

The combination of the intensity and width changes of peak-4 results in a substantial growth in the area of the peak (figures 8(a) and (b)) that displays an anti-correlation with the peak shift (figures 6(a) and (b)). It therefore seems feasible that there is a change in the physical properties that could relate to the transformation of the network, which is discussed in section 4.2. The pattern for the heating cycle does not exactly follow that of the cooling cycle but does reproduce the sharp change in position for the temperature region above 200 K. This conjecture can only be investigated further through a study of the proton dynamics by spectroscopic techniques. NMR studies of the proton relaxation have suggested that the disordered component has substantial rotational mobility such that it can be classed as 'plastic ice', converting (reversibly) to a brittle ice at low temperatures (Liu *et al* 2006, Seyed-Yazdi *et al* 2008a, Webber *et al* 2007a, 2007b). The area of peak-4 increases significantly and reversibly as the temperature is lowered, and may correspond to temperature modification of the disordered hydrogen-bond network. The small reduction in the area of peak 2 just prior to melting may be an observation of a pre-melting phenomenon.

The widths of the composite peaks for the crystalline components give information about the diffraction broadening that may be related to the crystallite size through the Scherrer equation. The D20 instrumental resolution at these Q values is around 0.012 ± 0.002 Å^{-1}. However, the fitted parameters shown in table 1 indicate that, although the widths for the confined ice remain relatively constant with respect to temperature, they have a number of different values. Under these conditions it is not possible to evaluate an overall pore size as the results imply that there is possibly some orientational correlation of the crystal axes with the pore axis, indicating that the crystallites could be needle-like in shape. Alternatively, the variation could arise from the particular nature of the stacking faults. This is an interesting observation but a full interpretation is beyond the scope of the present paper and will require detailed evaluation by computer modelling (Hansen *et al* 2007).

The origin of peak-2 is less easy to ascertain, although it has been observed as a specific feature in separate studies of ice in a sol–gel silica (Baker, Dore, unpublished data). It is a 'partially-broadened' peak at ∼1.69 Å^{-1} that occurs between the first two peaks of the hexagonal ice triplet. In simple terms, it would correspond to a short-range periodicity of 3.7 Å that does not seem to relate directly to the usual features of a hydrogen-bonded network of either crystalline or amorphous nature. It is possible that it might be an indication of a modified structure of water/ice at the silica interface. At present, it is impossible to identify the reason for this contribution although it is possible that it will be explained later when detailed simulation studies are conducted. It is well known that many different geometric arrangements can be created for a hydrogen-bonded assembly, either through ice polymorphs (Henry *et al* 2005) or alternatively through local cluster formation (Xenides *et al* 2006). There are two other possible reasons for the presence of this peak. The first concerns the water–silica interaction and the cross-correlation terms across the interface. The evaluation of the water/ice diffraction pattern is based on the subtraction of the 'dry' silica pattern from the 'wet' silica pattern and this does not eliminate the cross-correlation terms that involve features from the water–silica correlations. With large pore sizes, as used here, it is usual to assume that these terms make a negligible contribution as they only involve the short-range effects at the interface. Furthermore, the silica is of an amorphous form so that direct registry with the crystalline ice lattice is unlikely and any sharp features in the diffraction pattern would not normally be expected. However, the lower temperature and the associated reduction of molecular mobility could affect the local correlations of the interfacial hydrogen-bonded structures, involving surface siloxyl groups and neighbouring water molecules that are dependent on the local environment at the ice–silica interface. It is known that the internal surface of the cylindrical pores in SBA-15 silicas has a microporous corona that influences some of the properties revealed in gas adsorption (Joo *et al* 2002) or DSC and SANS studies (Schreiber *et al* 2001, 2006) It is therefore possible that this effect could be responsible for the 'additional' peak in the decomposition of the intensity profile, as the water/ice would be in a different environment to the rest of the sample. However, the size of the contribution to the profile seems to be too large for this explanation to be feasible unless the structural modification extends into the central region of the pore.

A mono-molecular layer structure at a smooth interface would exhibit considerable diffraction broadening and would not be easily identified in the diffraction pattern. Nevertheless,

it is feasible that a constrained ice-like layer could be formed at the interface, which has some extension along the length of the pores to create a two-dimensional crystalline sheet (Inaba *et al* 2005). If so, such an extended structure would give a peak that would be expected to exhibit an asymmetric profile but unfortunately this effect cannot be isolated from the experimental data due to the presence of overlapping peaks. Furthermore, the parameter values describing the temperature variation appear to vary in a similar manner to the crystalline component, which would not be expected for a layer firmly localized and in contact with the walls of the silica substrate. The possible presence of a microporous halo in the pores of the SBA-15 silica is similarly unlikely to give this effect. The second possibility is that there is a modified form of crystalline ice that could be created at the grain boundaries of the crystallite assembly. Although this would explain the associated expansion with temperature change, it would also indicate the presence of a very large amount of material between the crystallites in addition to the amorphous ice component. Furthermore, it would be expected that the subsequent growth of the crystalline component would result in a decrease of this contribution, which is not observed. Consequently, it is difficult to provide a satisfactory explanation for the presence of peak-2 in the observations. However, the curve-fitting process indicates that the observed profile cannot be solely due to an asymmetric shape to peak 1. It is hoped that the study of partially-filled samples ($f = 0.6$ and 0.4) will help to provide an answer to this question; this work is in progress and will be reported later as Paper 4 in the series.

4.2. Co-existence of ice structures

The interpretation of the results presented in the previous section emphasizes the complexity of the nucleation and growth processes occurring in the confined water/ice state. The analysis also seems to indicate a slight variation for the data obtained between the fast and slow runs although the overall features of the diffraction pattern remain remarkably similar. One obvious change that is apparent in the raw data is the magnitude of peak-5, which is significantly reduced for the slow run. This behaviour has been discussed in Paper 2 as a possible expulsion of the pore water during the temperature changes but an alternative explanation may need to be considered. Johari has considered the inter-relationship of hexagonal and cubic ice using thermodynamic arguments (Johari 2005) and he concludes that the 'balance' between the two states can be influenced by the cooling rate. It is probably premature to associate the behaviour observed in the present experiment with this prediction but the results are indicative of some variation that will require more detailed investigation.

In conclusion, the results indicate that several defective ice states contribute to the measured diffraction pattern for the nucleated solid phase of water in confined geometry. Each of the composite ice phases is also observed to change systematically with temperature over the range 256–204 K (fast run) and 257–102 K (slow run), indicating that all components increase as the temperature reduces. Peak-4, corresponding to ida ice, is found to have an anomalous behaviour concerning the displacement of the peak position. The change in the position of this peak is clearly identified (figure 6) over the range 225–205 K for all the runs (heating and cooling) and suggests a significant reversible modification of the amorphous/disordered component in this temperature regime. It presumably relates to certain dynamic features of the hydrogen-bonded assembly that contribute to the observed structural characteristics. Prior work by NMR relaxation has indicated that the disordered component may be characterized as ice in a predominantly rotator (or plastic) state. (Liu *et al* 2006, Webber *et al* 2007a, 2007b, Webber and Dore 2008). In the same way that the diffraction data indicates that a disordered component converts to cubic ice (and some hexagonal ice) over a temperature range from the melting point down to below 200 K, the NMR work shows that there is a conversion over a similar temperature range of a rotationally mobile component, with a transverse relaxation time T_2 of around 100–200 μs, to brittle ice, with a T_2 of around 10 μs. It is impossible at this stage to say whether the observed changes may be described as predominantly due to changes in the rotational or translational characteristics of the 'plastic' ice and its conversion to a brittle ice; more information is needed on how this rotational and translation motion changes with temperature. The fractional amounts that convert, as measured by the two different techniques, are in good agreement. An alternative explanation that might be favoured by some researchers is that the system represents an extreme super-cooling of a highly viscous phase of water that undergoes a glass transformation to an intermediate density ice. However this data offers no evidence to support the concept of a liquid–liquid transition in this temperature region. Further work by spectroscopic techniques, such as NMR and QENS, will be needed to investigate the microscopic dynamics in more detail.

5. Summary

Several conclusions have been established from the curve-fitting techniques used to analyse the profile of the triplet ice peak in the 86 Å pores:-

- nucleation from the liquid phase creates a mixture that incorporates hybrid crystallites of ice-I_h and ice-I_c with an intermediate density (ida) form of amorphous ice,
- the amount of crystalline and amorphous material grows during a cooling run and reduces during a heating run; the changes are reversible and hysteresis effects are relatively small,
- an analysis based on facetted growth in the pore volume leading to three asymmetric peak profiles is not able to give a satisfactory fit to the data.
- an analysis based on a set of five symmetric peaks is preferred, giving three sharp peaks correspond to the crystalline phases of ice-I_h, one to the presence of ida ice and one that cannot be assigned to any specific structure,
- there are small variations in the components of the profile that appear to be dependent on the rate of cooling/heating. The parameter values describing the variation with

temperature are found to vary in a systematic and smooth manner.

These results suggest that the phase relationship of ices in confined geometry is more complex than has been previously realized. The data indicate the co-existence of several different structural phases of ice but it is not possible to comment on the precise location of these inhomogeneities inside the pore volume. Further work is in progress relating to partially-filled pores for the same SBA-15 silica sample and will be reported in a later publication (Seyed-Yazdi *et al* 2008b).

Acknowledgments

The silica samples were fabricated in Berlin as a part of a research programme supported by the Deutsche Forschungsgemeinschaft in the framework of the SFB 448 'Mesoscopically Organized Composites'. We are indebted to Dr Sylvia Reinhard (Technical University Berlin) for the preparation of the SBA-15 sample and to Dr Alan Evans (University of Kent) for providing the NonLinReg program used in the analysis. The experimental measurements were carried out at the Institut Laue-Langevin with the support of the EPSRC (UK); we wish to thank Thomas Hansen for his invaluable assistance during the experimental work. One of us (JBWW) was partially supported by collaborations with the BMFFFS Project (Behaviour and Modelling of Faults/Fractures/Fluids Systems) and the Centre for Gas Hydrate Research, both in the Institute of Petroleum Engineering, Heriot-Watt University, and is currently partially supported by EPSRC grant EP/D052556/1. One of us (JS-Y) wishes to thank the Iranian Ministry of Science and Technology and the British Council for a grant to enable her to visit to the University of Kent, during which the analysis was conducted.

Appendix A. A skew function to model asymmetric peaks

The introduction of a skew effect into the peak profile can be achieved by modifying the argument in the 'cosh' expression. The measurements indicate an apparent asymmetry such that the peak has a sharper rise at low Q-values and a significant broad 'tail' at high Q-values. The extent of the asymmetry may be determined by a new parameter 'ε', which produces a skew towards the high-Q values for 'ε', positive and to low-Q values for 'ε', negative. The most convenient parametric representation has been found to be through the use of a function defined by:-

$$I(Q,i) = \frac{I_0(i)}{F(Q,\varepsilon;i)} \tag{2}$$

with:-

$$F(Q,\varepsilon) = \cosh\left\{\left[1 - \tanh(\varepsilon^2) \times \tanh\left(\frac{Q-Q_0}{\sigma_\varepsilon}\right)\right]\left(\frac{Q-Q_0}{\sigma}\right)\right\} \tag{3}$$

in which the parameter values, relate to the position, width and asymmetry features of the peak. In this form, Q_0 is the peak position and σ is the peak width, as previously. The additional parameters introduce an asymmetry parameter, ε, with an associated width given by σ_ε. The parameter value, ε^2, is constrained to be positive so that the function has an asymmetric form in which the 'tail' is on the positive side of the peak. In the simplest case it is possible to set σ equal to σ_ε.

The overall triplet profile is obtained as the summation of three asymmetric peaks in which each peak is characterized by one linear coefficient, I_0, and four nonlinear coefficients, ε^2, σ_ε, Q_0 and σ. Using three independent peaks therefore gives a total of 15 variable parameters. However, structural constraints and the relative insensitivity of parameters defining the small third peak already fix several of the variables to a small range of possibilities. This functional form is not identical to that arising in the Warren profile expressions but is a convenient parametric representation that is able to represent the asymmetric nature of the peaks in a convenient way for the profile analysis.

Appendix B. A brief summary of the structure of amorphous ices

Extensive neutron and x-ray studies have been made on the various forms of amorphous ice that are usually classified as either low-density amorphous ice (lda), high-density amorphous ice (hda) or very high density amorphous ice (Loerting *et al* 2001, Finney *et al* 2002b). The hda form is produced by 'pressure amorphization' of hexagonal ice at low temperature (77 K). It converts to a form of lda ice at 145 K for H_2O and 140 K for D_2O. The most usual way of creating lda ice is by vapour-deposition onto a cold substrate plate (Chowdhury *et al* 1982) or alternatively by the hyper-quenching of water droplets (Loerting *et al* 2001). These methods result in several minor variants of the 'neat' lda ice, as revealed in the x-ray or neutron diffraction patterns and sometimes referred to as amorphous solid water (ASW). The small structural variations seem to depend on various parameters such as the precursor material (water droplets, vapour or hda ice), the temperature of formation/conversion, etc but it seems probable that a common structure is created after annealing at ∼120–130 K. Experimental studies show that the conversion of lda ice to 'defective cubic' ice occurs at 140 K for pure D_2O samples (Blakey 1994) but the transition temperature is considerably raised if there is any occluded gas (Davies 1992). It is, however, notable that computational studies (Guillot and Guissani 2003) indicate that there are small structural variations, depending on the temperature history of the sample, giving distinct forms of lda_I and lda_{II} ice.

Spectroscopic studies suggest that all the water molecules are fully-hydrogen-bonded and the structural modelling of the diffraction data appears to confirm this assertion (Dore and Blakey 1995). Consequently, the annealed low-density form of amorphous ice (lda) may be characterized as a fully hydrogen-bonded random network with four-fold co-ordination. More recent studies using H/D isotopic substitution have confirmed

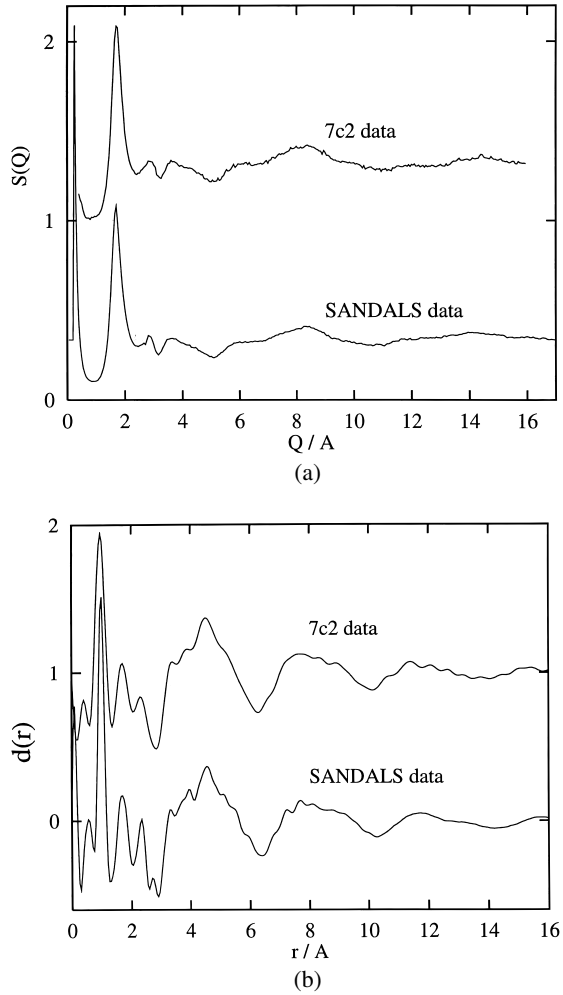

Figure B.1. Comparison of (a) differential scattering cross-sections and (b) radial density distributions of a-D_2O from 7C2 and SANDALS.

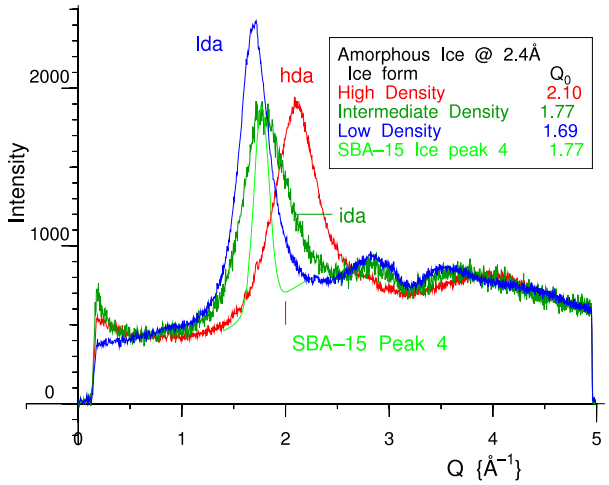

Figure B.2. Diffraction patterns for Ida, ida and hda ices, as well as that of peak 4 for the ice in the SBA-15 sample.
(This figure is in colour only in the electronic version)

these general principles. The formation of vhda ice (Finney *et al* 2002a) suggests that the hda form may not be a specific phase with a well-defined structure and that a series of ices with variable high densities may exist. There remains an active debate about the relevance of this phase to the polyamorphism of the amorphous ices with an on-going controversy about the phase transformations and the existence of a second critical point (Poole *et al* 1992).

For the lda ice form, the local environment round each water molecule retains an approximate tetrahedral conformation through two-proton donor and two-proton acceptor bonds to four neighbouring water molecules and is therefore similar to that of either hexagonal or cubic ice. The difference in structure occurs in the positions of the second H-bonded neighbour molecule corresponding to the intermediate range of 4–10 Å that creates the network connectivity with five and seven-fold rings additional to the six-fold rings of the crystalline form (Boutron and Alben 1975). It seems that this general structure is reproducible from several different production routes although recent studies (Loerting *et al* 2001) have indicated that there may be some small differences that depend on the thermal history of the sample.

Diffraction studies of vapour-deposited D_2O ice have been reported (Blakey 1994) using reactor and pulsed neutron techniques. The results are shown for both experiments in figure B.1. The main peak occurs at a Q-value of 1.715 ± 0.005 Å^{-1} and is therefore close to the central peak of the hexagonal ice triplet at $\sim$1.75 Å^{-1}. Since the current data for ice in the SBA silica sample, shown in figure 3, overlap this region, it is not easy to separate out the two components. However, it can also be seen that there is a subsidiary oscillation in the region of 2.8 Å^{-1} that corresponds approximately with the emergence of a broad peak in the data for the confined ice. Furthermore, the general diffuse scattering beyond the main peak is an indication that some form of disorder must be present. Koza *et al* (2006) have investigated the transformation of hda ice to lda ice and shown that there is a continuous displacement of the main peak, indicating the formations of intermediate states rather than a simple two-phase process. However, the main peaks of lda, ida and hda ices are much broader than that of the ice in the SBA sample as shown by the superimposed diffraction patterns in figure B.2 (the ida ice pattern has been chosen to have the same position as peak 4 in the fitted data shown in figure 3). These preliminary comparisons suggest that there is no discernible isolated lda ice phase present in the SBA-15 pores, but imply that the type of disorder arising from the distortion of the network connectivity (due say to surface effects in pores) could have an influence on the defective crystalline form.

The apparent discrepancy in the peak positions for the present data and those extracted from the fitted parameters implies the existence of a modified form of amorphous ice. The shift from 1.708 to 1.748 Å^{-1} suggests that the spatial correlations contract by $\sim$2.4% and the density therefore increases by approximately 8%. Although it must be remembered that the peak position is not solely affected by the density. The possible existence of an intermediate density form of amorphous ice has been proposed by several groups and some of the temperature-dependent effects for

the water and ice phases quantified (Urquidi *et al* 2004). A more detailed consideration of this possibility will be presented separately when the additional measurements for the partially-filled samples are fully analysed. Other work (Zanotti *et al* 2005) on water/ice in Vycor for an extremely low filling-factor (monolayer coverage, at $f = 0.25$ hydration) has indicated the formation of lda ice. Some recent results (Jalassi *et al* 2008) have indicated that lda ice may also be formed in low coverage studies ($f = 0.3$) of water/ice in a super-microporous SPS-1 silica (Bagshaw and Hayman 2001a, 2001b). It therefore seems that amorphous ices formed in confined geometry may be stable at much higher temperatures than in the bulk state. Further work is in progress to investigate these features and to characterize the ice created under different conditions.

References

Bagshaw S A and Hayman A R 2001a *Adv. Mater.* **13** 1011

Bagshaw S A and Hayman A R 2001b *Micropor. Mesopor. Mater.* **44** 81–8

Baker J M 1996 *PhD Thesis* Physics, University of Kent at Canterbury, UK

Baker J M, Dore J C and Behrens P 1997 *J. Phys. Chem.* B **101** 6226–9

Bellissent-Funel M C, Sridi-Dorbez R and Bosio L 1996 *J. Chem. Phys.* **104** 10023–9

Blakey D M 1994 Structural studies of vapour-deposited amorphous–ice and argon/amorphous-ice systems by neutron diffraction *PhD Thesis* Physics, University of Kent at Canterbury, UK

Boutron P and Alben R 1975 *J. Chem. Phys.* **62** 4848–53

Chowdhury M R, Dore J C and Wenzel J T 1982 *J. Non-Cryst. Solids* **53** 247–65

Davies E 1992 *PhD Thesis* University of Kent

Dore J, Webber B, Montague D and Hansen T 2004 *Novel Approaches to the Structure and Dynamics of Liquids: Experiments, Theories and Simulations* ed J Samios and V A Durov (Netherlands: Kluwer–Academic) pp 143–56

Dore J C and Blakey D M 1995 *J. Mol. Liq.* **65/66** 85–90

Ergun S 1970 *J. Appl. Crystallogr.* **3** 153

Evans W A B 1997 *Advanced Numerical Techniques* (Canterbury: University of Kent) (Course notes and private communication)

Finney J L, Bowron D T, Soper A K, Loerting T, Mayer E and Hallbrucker A 2002a *Phys. Rev. Lett.* **89** 205503

Finney J L, Hallbrucker A, Kohl I, Soper A K and Bowron D T 2002b *Phys. Rev. Lett.* **88** 225503

Guillot B and Guissani Y 2003 *J. Chem. Phys.* **119** 11740–52

Hansen T C, Falenty A and Kuhs W F 2007 *Physics and Chemistry of Ice* ed W F Kuhs (Cambridge: RSC Publishing) pp 201–8

Hansen T C, Koza M M and Kuhs W F 2008 *J. Phys.: Condens. Matter* **20** at press

Henry M, Bogge H, Diemann E and Muller A 2005 *J. Mol. Liq.* **118** 155–62

Inaba A, Sakisato N, Bickerstaffe A K and Clarke S M 2005 *J. Neutron Res.* **13** 87–90 http://search.ebscohost.com/login.aspx?direct=true&db=aph&AN=16072087&site=ehost-live

Jalassi J, Dore J C, Webber J B W and Bellissent-Funel M C 2008 in preparation

Johari G P 2005 *J. Chem. Phys.* **122** 194504

Joo S H, Ryoo R, Kruk M and Jaroniec M 2002 *J. Phys. Chem.* B **106** 4640–6

Koza M M, Hansen T, May R P and Schober H 2006 *J. Non-Cryst. Solids* **352** 4988–93

Kuhs W F 1998 private communication

Liu E, Dore J C, Webber J B W, Khushalani D, Jähnert S, Findenegg G H and Hansen T 2006 *J. Phys.: Condens. Matter* **18** 10009–28

Loerting T, Salzmann C, Kohl I, Mayer E and Hallbrucker A 2001 *Phys. Chem. Chem. Phys.* **3** 5355–7

Morishige K and Uematsu H 2005 *J. Chem. Phys.* **122** 044711

Poole P H, Sciortino F, Essmann U and Stanley H E 1992 *Nature* **360** 324–8

Schreiber A, Ketelsen I and Findenegg G H 2001 *Phys. Chem. Chem. Phys.* **3** 1185–95

Schreiber A, Ketelsen I, Findenegg G H and Hoinkis E 2006 *Characterization of Porous Solids* (*Studies in Surf. Sci. and Catalysis.* vol 7) ed P L Llewellyn, J Rouguerol, F Rodrigues-Reinosi and N A Seaton (Amsterdam: Elsevier) pp 17–24

Seyed-Yazdi J, Dore J C, Webber J B W, Findenegg G H and Hansen T 2008a *J. Phys.: Condens. Matter* **20** 205107

Seyed-Yazdi J, Farman H, Dore J C, Webber J B W and Findenegg G H 2008b in preparation

Steytler D C and Dore J C 1985 *Mol. Phys.* **56** 1001–15

Steytler D C, Dore J C and Wright C J 1983a *Mol. Phys.* **48** 1031–51

Steytler D C, Dore J C and Wright C J 1983b *J. Phys. Chem.* **87** 2458–9

Szczygielska A, Burian A and Dore J C 2001 *J. Phys.: Condens. Matter* **13** 5545–61

Urquidi J, Benmore C J, Egelstaff P A, Guthrie M, Mclain S E, Tulk C A, Klug D D and Turner J F C 2004 *Mol. Phys.* **102** 2007–14

Warren B E and Bodenstein P 1965 *Acta Crystallogr.* **18** 282

Warren B E and Bodenstein P 1966 *Acta Crystallogr.* **20** 602

Webber B and Dore J 2004 *J. Phys.: Condens. Matter* **16** S5449–70 (Special Issue: Water in Confined Geometry)

Webber J B W, Anderson R, Strange J H and Tohidi B 2007a *Magn. Reson. Imaging* **25** 533–6

Webber J B W and Dore J C 2008 *Nucl. Instrum. Methods* A **586** 356–66

Webber J B W, Dore J C, Strange J H, Anderson R and Tohidi B 2007b *J. Phys.: Condens. Matter* **19** 415117

Xenides D, Randolf B R and Rode B M 2006 *J. Mol. Liq.* **123** 61–7

Zanotti J M, Bellissent-Funel M C and Chen S H 2005 *Europhys. Lett.* **71** 91–7